



Contents lists available at ScienceDirect



# Catalysis Today

journal homepage: [www.elsevier.com/locate/cattod](http://www.elsevier.com/locate/cattod)

## TiO<sub>2</sub> photocatalysis of 2-isopropyl-3-methoxy pyrazine taste and odor compound in aqueous phase: Kinetics, degradation pathways and toxicity evaluation

M. Antonopoulou, I. Konstantinou\*

Department of Environmental and Natural Resources Management, University of Patras, 30100 Agrinio, Greece

### ARTICLE INFO

#### Article history:

Received 14 January 2014

Received in revised form 10 March 2014

Accepted 13 March 2014

Available online xxx

#### Keywords:

Taste and odor

TiO<sub>2</sub>

Photocatalysis

Transformation products

Scavengers

### ABSTRACT

In recognition of the growing demand regarding the control of undesired taste and odor (T&O) problems in natural water resources, the photocatalytic degradation of 2-isopropyl-3 methoxy pyrazine (IPMP), a common metabolite of soil actinomycetes which contributes a rotten vegetable odor to water, was investigated under simulated solar irradiation. Under the studied conditions ( $C = 10 \text{ mg L}^{-1}$ ,  $C_{\text{TiO}_2} = 100 \text{ mg L}^{-1}$  and  $I = 600 \text{ W m}^{-2}$ ), 95% of IPMP was removed within 20 min of irradiation. The reaction intermediates were completely mineralized to CO<sub>2</sub> and the nitrogen was predominantly released as NH<sub>4</sub><sup>+</sup> ions after 240 min irradiation. The major transformation products of TiO<sub>2</sub> photocatalysis of IPMP have been determined by the use of high resolution accurate liquid chromatography–orbitrap mass spectrometry as well as gas chromatography–mass spectrometry (GC–MS) techniques. Hydroxylation of the isopropyl and methoxy groups has been identified as the main reaction pathway. Scavenging experiments indicated the important role of HO<sup>•</sup>, h<sup>+</sup> and O<sub>2</sub><sup>•-</sup> in the photocatalytic process. Toxicity assessment revealed the efficiency of the photocatalytic treatment to achieve almost complete detoxification of the irradiated solution.

© 2014 Elsevier B.V. All rights reserved.

### 1. Introduction

The increasing occurrence of taste and odor (T&O) compounds in drinking water supplies has been recognized as an important water quality problem receiving substantial public concern throughout the world [1]. Although, changes in esthetic values are typically not problematic from toxicological points of view, they impose serious considerations for the quality of drinking water [2]. A great number of organic compounds either naturally occurring in aquatic compartments or from industrial sources, or even produced during water treatment, can cause undesirable tastes and odors in drinking water in extremely low concentrations. Of particular importance is the group of naturally occurring compounds that produce earthy–musty odors in drinking water [3].

In general, the removal of the majority of T&O compounds from drinking water is a difficult task since their odor threshold is extremely low, usually in the range of ng L<sup>-1</sup> [4]. Their incomplete removal in potable water by conventional treatment processes in combination with the growing demand for good quality

clean water has led to the development of alternative more efficient water treatment processes [4,5]. In last decades, heterogeneous photocatalytic process employing catalysts such as TiO<sub>2</sub>, has demonstrated promising results for the degradation of different taste and odor compounds. However, only the photocatalytic removal 2-methylisoborneol and geosmin is extensively documented in the literature [6–9]. Among T&O compounds, we have focused on IPMP, a representative compound of the group of naturally occurring compounds that produce earthy–musty odors in drinking water. IPMP is a metabolite of soil actinomycetes which contributes a rotten vegetable odor to water and has been frequently found in natural water serving as drinking water resources. Although this compound does not have a direct negative effect on the public health, its presence, even at trace levels, gives rise to esthetic issues due to its low threshold of 0.2 ng L<sup>-1</sup> [1]. According to our knowledge this is the first research article of the current state of knowledge regarding the application of the heterogeneous photocatalysis for the removal of IPMP from aqueous phase. Thus, the aim of this work is to comprehensively study and evaluate the application of TiO<sub>2</sub> photocatalysis for the treatment of IPMP. In this context, the main aspects investigated have been: the efficiency of TiO<sub>2</sub> photocatalytic process for IPMP degradation, the identification of transformation products (TPs) of IPMP, the elucidation of

\* Corresponding author. Tel.: +30 2641074186.

E-mail addresses: [iokonst@upatras.gr](mailto:iokonst@upatras.gr), [iokonst@cc.uoi.gr](mailto:iokonst@cc.uoi.gr) (I. Konstantinou).

mechanistic details of the photocatalytic reaction using scavenging experiments, the evaluation of mineralization as well as the toxicity evolution during the process.

## 2. Experimental

### 2.1. Reagents and materials

IPMP, analytical grade >98%, was purchased from TCI (TOKYO Chemical Industry CO.). Titanium dioxide P25 from Degussa (Germany) was used as photocatalyst. HPLC grade solvents (acetonitrile, isopropanol and methanol) were supplied by Merck (Darmstadt, Germany). Sodium azide ( $\text{NaN}_3$ ), potassium iodide (KI) and *p*-benzoquinone (BQ) were obtained from Sigma-Aldrich. Ultrapure water was obtained from a Millipore Waters Milli-Q water purification system.

### 2.2. Photocatalytic degradation experiments

Photocatalytic experiments were carried out in a solar simulator Atlas Suntest XLS+ (Germany). Illumination was provided with a xenon lamp (2.2 kW) which was jacketed with special filters restricting the transmission of wavelengths below 290 nm. Irradiation experiments were performed using a Pyrex glass UV-reactor containing 250 mL of aqueous solutions and the appropriate amount of  $\text{TiO}_2$  ( $100 \text{ mg L}^{-1}$ ) at natural pH. The suspension was kept in the dark for 30 min, prior to illumination to reach adsorption equilibrium onto semiconductor surface. A relatively low amount of  $\text{TiO}_2$  ( $100 \text{ mg L}^{-1}$ ) and a higher initial concentration of IPMP ( $10 \text{ mg L}^{-1}$ ) than the typical values found in drinking waters have been selected in the experiments in order to obtain slower kinetics and provide favorable conditions for the identification and structural elucidation of transformation products and the mineralization study.

### 2.3. Analytical procedures

#### 2.3.1. Kinetic study

IPMP concentrations were determined by a Dionex P680 HPLC chromatography equipped with a Dionex PDA-100 Photodiode Array Detector using a Discovery C<sub>18</sub>, (250 mm length  $\times$  4.6 mm ID, 5  $\mu\text{m}$  particle size) analytical column from Supelco (Bellefonte, PA, USA). The HPLC mobile phase was a mixture of LC-grade water pH 3 (30%) and acetonitrile (70%) with a flow rate of  $1 \text{ mL min}^{-1}$ . Column temperature was set at 40 °C. The detection of IPMP was performed at 212 nm.

#### 2.3.2. Mineralization studies

Total organic carbon (TOC) was measured on filtered suspensions (0.22  $\mu\text{m}$ ), using a Shimadzu TOC V-csh Analyzer equipped with a non-dispersive infrared detector.  $\text{NO}_3^-$  and  $\text{NO}_2^-$  ions, were determined by a Dionex ICS-1500 equipped with ASRS Ultra II self-regenerating suppressor.  $\text{NH}_4^+$  ions were analyzed by the colorimetric method based on indophenol blue formation [10] using an UV-vis spectrophotometer Hitachi, U-2000.

#### 2.3.3. Scavenging experiments for reactive species

The role of  $\text{HO}^\bullet$ ,  $\text{O}_2^\bullet^-$ ,  $\text{h}^\bullet$  and  ${}^1\text{O}_2$  in the reaction was determined with the addition of isopropanol ( $1000 \text{ mg L}^{-1}$ ), *p*-benzoquinone ( $20 \text{ mg L}^{-1}$ ), iodine anions ( $100 \text{ mg L}^{-1}$ ) and azide ( $10 \text{ mg L}^{-1}$ ) [11] to the solutions containing  $10 \text{ mg L}^{-1}$  IPMP, respectively. The employed concentrations were sufficient to inhibit the reactive species  $\text{HO}^\bullet$ ,  $\text{O}_2^\bullet^-$ ,  $\text{h}^\bullet$  and  ${}^1\text{O}_2$  as reported in previous works [11–13] using similar experimental conditions.

## 2.4. By products evaluation

### 2.4.1. LC-MS and GC-MS analysis

The intermediates generated during IPMP photocatalysis was characterized by an UPLC-ESI-MS system in positive ionization mode. The LC system was equipped with an Accela Autosampler, an Accela LC pump and a LIT Orbitrap mass spectrometer (Thermo Fisher Scientific, Germany). The chromatographic separations were run on a C18 Hypersil Gold, 100 mm  $\times$  2.1 mm i.d., 1.9  $\mu\text{m}$  particle size (Thermo Fisher Scientific, San Jose, USA), thermostated at 40 °C and the injection volume was 10  $\mu\text{L}$ . Mobile phases A and B were water/5 mM ammonium formate and methanol/5 mM ammonium formate, respectively, at a flow rate of  $300 \mu\text{L min}^{-1}$ . A linear gradient progressed from 90% A (initial conditions) to 0% A in 14 min, followed by a linear gradient to 90% A in 20 min. The ESI-source parameters were as follows: sheath and auxiliary gas flow rate 30 and 8 (nitrogen, arbitrary units), respectively; source voltage at 3.70 kV; capillary temperature was maintained at 320 °C. For fragmentation study, the voltage of the HCD collision cell was set at 35 eV. Prior to analysis, the orbitrap mass analyzer was externally calibrated, in the scan range  $m/z$  70–650, to obtain mass accuracy with  $\pm 5$  ppm. A resolving power of 60,000 was applied. Chemical compositions and accurate masses of the protonated molecules and their fragments were determined by means of chemical formula calculator, included in Xcalibur software. For the GC-MS analysis, the SPE method reported in an earlier study [11] was applied to the samples previous to the injection. GC-MS analysis was performed using a gas chromatograph-mass spectrometer (GC-MS), QP-2010 Shimadzu (Shimadzu, Kyoto, Japan). The GC-MS was equipped with a split/splitless auto-injector model AOC-20i and an auto sampler model AOC-20s. The GC was fitted with a fused silica capillary column SLB-5ms column (30 m  $\times$  0.25 mm and 0.25  $\mu\text{m}$  film thickness) from Supelco (Bellefonte, PA, USA). The operating chromatographic conditions were as follows: injector temperature 220 °C, column program of temperatures 50 °C (4 min) to 280 °C (2 min) at  $6^\circ\text{C min}^{-1}$  to 300 °C (2 min) at  $10^\circ\text{C min}^{-1}$ . Helium was used as the carrier gas at a flow rate of  $1.7 \text{ mL min}^{-1}$ . The ion source and transfer line were kept at 200 and 250 °C, respectively. The quadrupole mass spectrometer was operated in electron impact (EI) ionization mode at 70 eV and the spectra were obtained at a scan range from  $m/z$  50 to 450. The splitless mode was used for injection of 1  $\mu\text{L}$  volume.

### 2.5. Toxicity measurements

Acute toxicity of the treated samples was evaluated by monitoring changes in the natural emission of marine luminescence bacteria *Vibrio Fischeri*. The analysis was conducted by Microtox Model 500 Toxicity Analyzer (Azur Environmental). A briefly description of the procedure has been reported in our previous study [14].

## 3. Results and discussion

### 3.1. Kinetics of disappearance and mineralization by $\text{TiO}_2$ -photocatalytic process

Preliminary adsorption and photolysis experiments were carried out at the initial IPMP concentration of  $10 \text{ mg L}^{-1}$  to assess the extent of adsorption and photolysis of IPMP. Negligible adsorption of the target compound on the catalyst's surface was observed under dark conditions (data not shown). The direct photolysis (simulated solar radiation alone) showed that only 20% of IPMP was removed after 30 min of simulated solar illumination. However, after 4 h of irradiation almost 85% of the initial concentration of IPMP was degraded (Fig. 1). In contrast, no mineralization was

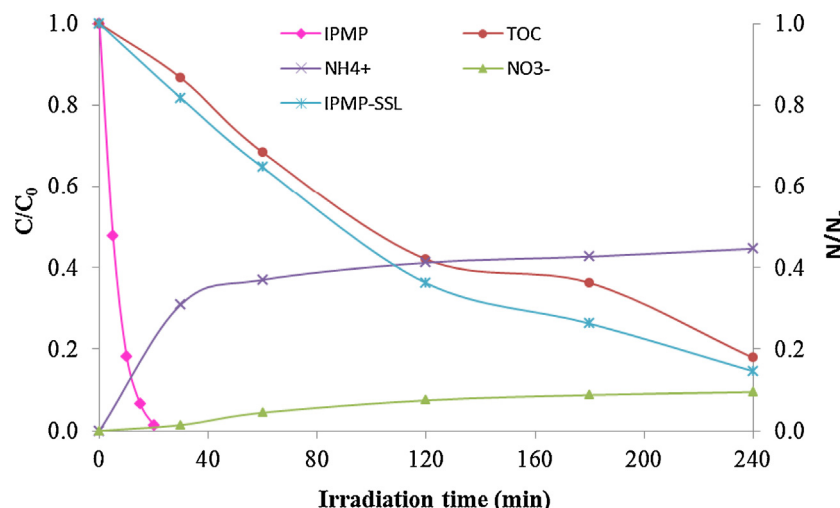


**Fig. 1.** Disappearance of IPMP, TOC removal and evolution of  $\text{NO}_3^-$  and  $\text{NH}_4^+$  ions under photolytic and photocatalytic conditions ( $[\text{IPMP}] = 10 \text{ mg L}^{-1}$ ,  $[\text{TiO}_2] = 100 \text{ mg L}^{-1}$ ,  $I = 600 \text{ W m}^{-2}$ ).

observed after the same irradiation time. Complete degradation of IPMP is rather a quick process and is achieved within 20 min in the presence of  $\text{TiO}_2$  with a half time of 3.3 min (Fig. 1) following apparent first-order kinetic model. Consequently, the decomposition that is observed in the presence of  $\text{TiO}_2$  is ascribed to the catalyst's activity. TOC removal followed a much slower rate compared to IPMP, showing a half time of 100.4 min following also first-order kinetics. High TOC removal percentages (approximately 80%) have been succeeded after 240 min irradiation. At the end of the process, nitrogen was mainly transformed into  $\text{NH}_4^+$  ions (45%) and in a lesser extent into  $\text{NO}_3^-$  (almost 10%).  $\text{NO}_3^-$  and  $\text{NH}_4^+$  ions reach about 55% of the expected stoichiometric nitrogen amount, indicating either that N-containing species remained adsorbed in the photocatalyst surface or that  $\text{NH}_3$  was produced and transferred to the gas phase. The lack of nitrogen stoichiometric recovery can be correlated with the remaining 20% of TOC indicating the presence of derivatives which still containing the organic nitrogen such as aliphatic amines (i.e. methylamine, ethylamine, dimethylamine, *n*-propylamine etc.) or intermediates bearing the C=N=C fragment arising from opening of pyrazine ring, as identified elsewhere [15,16]. In the present study, we focused on the characterization and identification of the primary TPs resulting from the photocatalytic degradation of IPMP. These primary TPs undergo ring opening, oxidation and demethylation mechanisms and finally transformed to lower molecular weight products before total mineralization. The higher amount of  $\text{NH}_4^+$  ions compared to  $\text{NO}_3^-$  is consistent with previous study that reported that the photocatalytic degradation of heterocyclic two-nitrogen containing compounds with a C=N=C fragment leads to the generation of a large amount of  $\text{NH}_4^+$  and a minor amount of  $\text{NO}_3^-$  [15].

### 3.2. Contribution of reactive species to photodegradation of IPMP

By using isopropanol, *p*-benzoquinone, iodine and azide ions as hydroxyl, superoxide anion, holes and singlet oxygen scavengers, respectively, the contribution of the reactive species on IPMP degradation was determined [11]. The pseudo-first order rate constants with or without the presence of the scavenging reagents are summarized in Table 1. The inhibitory effect was evaluated by the percent reduction of kinetic constants, denoted as %  $\Delta k$  in Table 1. The addition of isopropanol leads to almost completely inhibition on  $\text{TiO}_2$  photocatalytic degradation of IPMP (93.9% inhibition). Extensive inhibition of the process by isopropanol indicates the essential participation of  $\text{HO}^\bullet$  in the oxidation of IPMP. The addition

of iodine ions in the photocatalytic system provokes 91.2% inhibition at 30 min reaction with a calculated value of  $k = 0.0188 \text{ min}^{-1}$  (Table 1). Slightly lower inhibition of the degradation was observed compared to the inhibition in the presence of isopropanol ( $\text{HO}^\bullet$  radical scavenger) suggesting that reactions occur mainly at the surface of the photocatalyst via surface-bound  $\text{HO}^\bullet$  radicals and/or photo-generated holes. The addition of azide provokes partial inhibition of IPMP photocatalytic degradation as shown in Table 1 (around 62% inhibition). Moreover, when *p*-BQ was added to the IPMP solution, 89.6% inhibition of IPMP photocatalytic degradation was observed, proving the significant contribution of  $\text{O}_2^\bullet-$  to the photocatalytic degradation of IPMP.

### 3.3. Identification of degradation products by mass spectrometric techniques

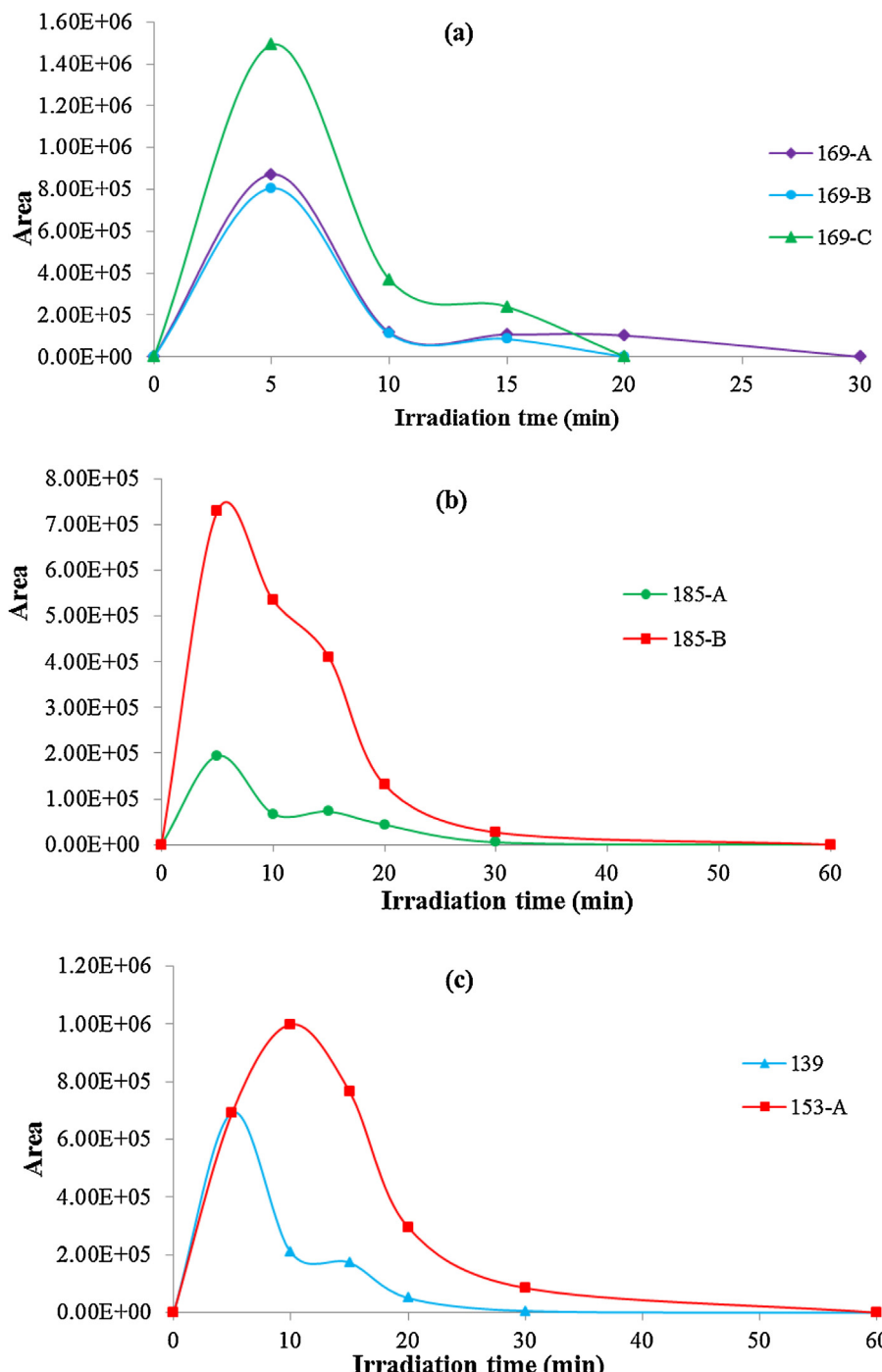
In photocatalytic processes, numerous intermediates and TPs can be formed as a consequence of the non-selectivity of  $\text{HO}^\bullet$  and the participation of the other photogenerated reactive species in various oxido-reductive reactions [17,18]. In some cases the transformation products can be more toxic and persistent than the parent compound [18] as well as can contribute to the organoleptic quality of the water [19]. This emphasize that the identification of transformation products is essential task in assessing the reliability of the degradation treatment for the pollutant and in optimizing the overall process efficiency. In the present study, identification and structural elucidation of intermediates is based on the use of accurate mass measurements,  $\text{MS}^2$ ,  $\text{MS}^3$  fragmentation and electron-impact mass spectra. The mass spectra characteristics of the detected TPs are presented in Tables 2 and 3 for HR-LC-MS and GC-MS analysis, respectively. TPs evolution as a function of irradiation time was also followed and the evolution profiles of the TPs are depicted in Fig. 2. Up to ten intermediate products were elucidated by high resolution accurate LC-MS analysis. Errors between the measured and the calculated accurate mass lower than  $\pm 5 \text{ ppm}$  were obtained in all cases providing a high degree of confidence in assigning the empirical formula and possible structures of the intermediates generated. Two TPs were identified by GC-MS through interpretation of the mass spectra and investigation of their characteristic ions as well as using the identification program of the NIST library with a fit value higher than 75%.

Three major monohydroxylated compounds with  $m/z$  169.0971 (A-C) were identified at the first stages of the photocatalytic reaction as a consequence of the non-selectivity of the  $\text{HO}^\bullet$

**Table 1**

Kinetic parameters (rate constants and % RSD, correlation coefficients ( $R^2$ ), half-lives ( $t_{1/2}$ )) of IPMP ( $10 \text{ mg L}^{-1}$ ) photocatalytic degradation in the presence of  $\text{TiO}_2$  suspension and with the addition of scavengers.

| Treatment system       | $k (\text{min}^{-1})$ (% RSD) | $t_{1/2} (\text{min})$ | $R^2$  | % $\Delta k$ |
|------------------------|-------------------------------|------------------------|--------|--------------|
| Control (no scavenger) | 0.2127 (0.9)                  | 3.3                    | 0.9779 |              |
| TOC                    | 0.0069 (12.2)                 | 100.4                  | 0.9736 |              |
| Isopropanol            | 0.0130 (11.9)                 | 53.3                   | 0.9886 | 93.9         |
| <i>p</i> -Benzoquinone | 0.0226 (7.7)                  | 30.7                   | 0.9890 | 89.4         |
| Iodine ions            | 0.0188 (8.1)                  | 36.9                   | 0.9916 | 91.2         |
| $\text{N}_3^-$         | 0.0806 (4.4)                  | 8.6                    | 0.9756 | 62.1         |

**Fig. 2.** Time evolution profiles of identified TPs based on HR-LC-MS data.

**Table 2**High resolution accurate mass data ( $[M + H]^+$ , MS<sup>2</sup>, MS<sup>3</sup> product ions, molecular formulas and relative error  $\Delta$ (ppm) for the identified transformation products.

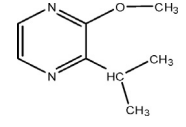
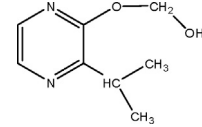
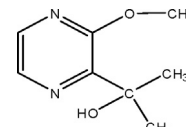
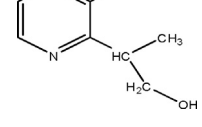
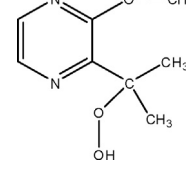
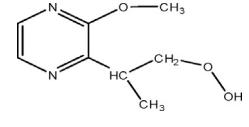
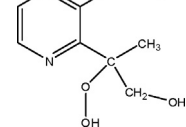
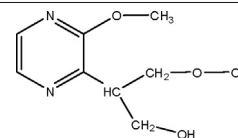
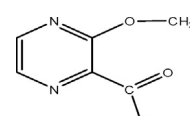
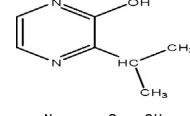
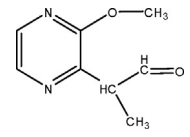
| $R_f$ | Molecular formula  | $[M + H]^+ m/z$     | $\Delta$ (ppm) | MS <sup>2</sup> $m/z$   | $\Delta$ (ppm) | MS <sup>3</sup>   | $\Delta$ (ppm) | Molecular structure   |
|-------|--|---------------------|----------------|---|----------------|---|----------------|---|
| 10.09 | C <sub>8</sub> H <sub>13</sub> N <sub>2</sub> O              | 153.1022<br>(IPMP)  | -0.590         | 138.0784<br>C <sub>7</sub> H <sub>10</sub> N <sub>2</sub> O<br>(-CH <sub>3</sub> ) (100)                                | -2.712         | 123.0550<br>C <sub>6</sub> H <sub>7</sub> N <sub>2</sub> O<br>(-CH <sub>3</sub> ) (100)               | -2.856         |    |
|       |  |                     |                | C <sub>7</sub> H <sub>13</sub> N <sub>2</sub> (-CO)<br>(30)   | -3.6226        |   |                |   |
|       |  |                     |                | 83.0597   | -4.6800        |   |                |   |
|       |  |                     |                | C <sub>4</sub> H <sub>7</sub> N <sub>2</sub><br>(-C <sub>4</sub> H <sub>5</sub> O) (20)                                 |                |   |                |   |
| 6.26  | C <sub>8</sub> H <sub>13</sub> N <sub>2</sub> O <sub>2</sub> | 169.0971<br>(169-A) | -4.697         | 151.0865<br>C <sub>8</sub> H <sub>11</sub> N <sub>2</sub> O<br>(-H <sub>2</sub> O) (100)                                | -0.791         | 136.0621<br>C <sub>7</sub> H <sub>8</sub> N <sub>2</sub> O<br>(-CH <sub>3</sub> ) (5)                 | -4.787         |    |
|       |  |                     |                |   |                | C <sub>6</sub> H <sub>7</sub> N <sub>2</sub> O<br>(-C <sub>2</sub> H <sub>4</sub> ) (100)             | -0.990         |   |
|       |  |                     |                |   |                | 119.0600  | -4.156         |   |
|       |  |                     |                |   |                | C <sub>7</sub> H <sub>7</sub> N <sub>2</sub><br>(-CH <sub>4</sub> O) (10)                             |                |   |
| 6.55  | C <sub>8</sub> H <sub>13</sub> N <sub>2</sub> O <sub>2</sub> | 169.0971<br>(169-B) | -4.970         | 151.0868<br>C <sub>8</sub> H <sub>11</sub> N <sub>2</sub> O<br>(-H <sub>2</sub> O) (100)                                | -0.003         | 136.0621<br>C <sub>7</sub> H <sub>8</sub> N <sub>2</sub> O<br>(-CH <sub>3</sub> ) (5)                 | -4.980         |    |
|       |  |                     |                |   |                | C <sub>6</sub> H <sub>7</sub> N <sub>2</sub> O<br>(-C <sub>2</sub> H <sub>4</sub> ) (100)             | -2.352         |   |
|       |  |                     |                |   |                | 119.0600  | -2.980         |   |
|       |  |                     |                |   |                | C <sub>7</sub> H <sub>7</sub> N <sub>2</sub><br>(-CH <sub>4</sub> O) (10)                             |                |   |
| 7.44  | C <sub>8</sub> H <sub>13</sub> N <sub>2</sub> O <sub>2</sub> | 169.0971<br>(169-C) | -4.460         | 151.0864<br>C <sub>8</sub> H <sub>11</sub> N <sub>2</sub> O<br>(-H <sub>2</sub> O) (100)                                | -0.394         | 123.0550<br>C <sub>6</sub> H <sub>7</sub> N <sub>2</sub> O<br>(-C <sub>2</sub> H <sub>4</sub> ) (100) | -2.514         |  |
|       |  |                     |                |   |                | C <sub>7</sub> H <sub>9</sub> N <sub>2</sub><br>(-CH <sub>2</sub> O) (20)                             | 0.703          |   |
|       |  |                     |                |   |                | 119.0600  | 1.468          |   |
|       |  |                     |                |   |                | C <sub>7</sub> H <sub>7</sub> N <sub>2</sub><br>(-CH <sub>4</sub> O) (10)                             |                |   |
| 6.76  | C <sub>8</sub> H <sub>13</sub> N <sub>2</sub> O <sub>3</sub> | 185.0921<br>(185-A) | -4.586         | 167.0813<br>C <sub>8</sub> H <sub>11</sub> N <sub>2</sub> O <sub>2</sub><br>(-H <sub>2</sub> O) (40)                    | -1.521         |   |                |  |
|       |  |                     |                | 124.0628<br>C <sub>6</sub> H <sub>8</sub> N <sub>2</sub> O<br>(-C <sub>2</sub> H <sub>5</sub> O <sub>2</sub> )<br>(100) | -1.809         |   |                |   |
| 7.05  | C <sub>8</sub> H <sub>13</sub> N <sub>2</sub> O <sub>3</sub> | 185.0921<br>(185-B) | -4.211         | 151.0865<br>C <sub>8</sub> H <sub>11</sub> N <sub>2</sub> O<br>(-H <sub>2</sub> O <sub>2</sub> ) (100)                  | -0.725         | 123.0549<br>C <sub>6</sub> H <sub>7</sub> ON <sub>2</sub><br>(-C <sub>2</sub> H <sub>4</sub> ) (100)  | -3.246         |  |
|       |  |                     |                | 138.0787<br>C <sub>7</sub> H <sub>10</sub> N <sub>2</sub> O<br>(-CH <sub>3</sub> O <sub>2</sub> ) (40)                  | -0.684         |   |                |   |
| 4.13  | C <sub>8</sub> H <sub>13</sub> N <sub>2</sub> O <sub>4</sub> | 201.0869<br>(201-A) | -5.238         | 183.0755<br>C <sub>8</sub> H <sub>11</sub> N <sub>2</sub> O <sub>3</sub><br>(-H <sub>2</sub> O) (40)                    | -5.000         | 97.0757<br>C <sub>5</sub> H <sub>9</sub> N <sub>2</sub><br>(-CH <sub>3</sub> OH)<br>(100)             | -3.244         |  |
|       |  |                     |                | 129.1018<br>C <sub>6</sub> H <sub>13</sub> N <sub>2</sub> O<br>(-C <sub>2</sub> O <sub>2</sub> ) (100)                  | -5.000         |   |                |   |
|       |  |                     |                | 157.0970  | -1.172         |   |                |   |
|       |  |                     |                | C <sub>7</sub> H <sub>13</sub> N <sub>2</sub> O <sub>2</sub><br>(-CO <sub>2</sub> ) (25)                                |                |   |                |   |

Table 2 (Continued)

| $R_t$ | Molecular formula  | [M + H] <sup>+</sup> $m/z$ | $\Delta$ (ppm) | $MS^2 m/z$  | $\Delta$ (ppm) | $MS^3$   | $\Delta$ (ppm) | Molecular structure   |
|-------|--|----------------------------|----------------|---|----------------|--|----------------|---|
| 4.45  | C <sub>8</sub> H <sub>13</sub> N <sub>2</sub> O <sub>4</sub> | 201.0869<br>(201-B)        | -5.218         | 183.0755<br>C <sub>8</sub> H <sub>11</sub> N <sub>2</sub> O <sub>3</sub><br>(-H <sub>2</sub> O) (40)                | -4.704         | 155.0819<br>C <sub>7</sub> H <sub>11</sub> N <sub>2</sub> O <sub>2</sub><br>(-CH <sub>2</sub> O <sub>2</sub> ) (100) | -4.185         |  |
|       |  |                            |                | 129.1017<br>C <sub>6</sub> H <sub>13</sub> N <sub>2</sub> O<br>(-C <sub>2</sub> O <sub>3</sub> ) (100)              | -4.180         |  |                |   |
|       |  |                            |                | 155.0819<br>C <sub>7</sub> H <sub>11</sub> N <sub>2</sub> O <sub>2</sub><br>(-CH <sub>2</sub> O <sub>2</sub> ) (35) | 2.811          |  |                |   |
| 5.52  | C <sub>7</sub> H <sub>9</sub> N <sub>2</sub> O <sub>2</sub>  | 153.0658                   | -4.600         |   |                |  |                |  |
| 5.01  | C <sub>7</sub> H <sub>11</sub> N <sub>2</sub> O              | 139.0866                   | -3.448         | 121.0756<br>C <sub>7</sub> H <sub>9</sub> N <sub>2</sub> (-H <sub>2</sub> O)<br>(100)                               | -3.427         |  |                |  |
| 5.44  | C <sub>8</sub> H <sub>11</sub> N <sub>2</sub> O <sub>2</sub> | 167.0807                   | -0.774         | 153.0664<br>C <sub>7</sub> H <sub>9</sub> O <sub>2</sub> N <sub>2</sub><br>(-CH <sub>2</sub> ) (100)                | -4.665         |  |                |  |

radical attack [11]. The formation of an intense product ion at  $m/z$  151.0865–151.0868 for all the isomers was observed, originating from H<sub>2</sub>O loss, well matched with OH group addition on the IPMP molecule. Through the analysis of their MS/MS spectra it could be proposed the position for hydroxyl group substitution. The absence of fragments which indicates modified pyrazine ring suggests the hydroxylation of either the isopropyl or methoxy chain. This assignment was further supported by the presence of a common fragment at  $m/z$  119.0600 which can be attributed to the loss of methanol and enabled the chemical modification of the pyrazine ring moiety to be excluded. A major fragment at  $m/z$  123.0550 occurs in the  $MS^3$  spectra of the three hydroxylated derivatives of pyrazine. This fragment corresponding to C<sub>6</sub>H<sub>7</sub>N<sub>2</sub>O could be attributed to the loss of the ethene. This can occur by hydrogen migration from the methoxy group to the tertiary carbon followed by loss of ethene [20]. As both isomers A and B show identical fragments corresponding to the loss of methyl group and methanol molecule, it is not possible to attribute the position of the hydroxyl group from  $MS^2$  and  $MS^3$  spectra. The absence of other product ions does not allow to distinguish these two hydroxyl TPs which can bear the hydroxyl on the methyl carbon of the methoxy group or on the tertiary carbon linked to the isopropyl group.

As regards isomer 169-C, the OH group is located on a terminal carbon of isopropyl chain, as assessed by the structural-diagnostic  $MS^3$  ion at  $m/z$  121.0762 which fit well with the loss of formaldehyde and by the absence of fragment at  $m/z$  136.0621, indicating the presence of a modified CH<sub>3</sub> group. The  $m/z$  121.0776 and the

corresponding loss of formaldehyde ion is a significant fragment only when a methoxy-group is situated in *ortho* position in relation to the alkyl side chain [20]. Similarly to our results, previous works on photocatalytic transformation of aromatic organic compounds bearing an isopropyl group have reported that, the attack of HO<sup>•</sup> radicals is favored on the isopropyl groups instead of the aromatic ring [21,22]. According to literature data single and multiple hydroxylation of the isopropyl group appeared to be kinetically favored in photocatalytic processes [21].

Two derivatives with [M + H]<sup>+</sup> ions at  $m/z$  185.0921 (185-A,B) were detected in 6.76 and 7.05 min (Table 2). By analyzing isomer 185-A, two main product ions at  $m/z$  167.0813 (loss of a water molecule) and  $m/z$  124.0628 (loss of C<sub>2</sub>H<sub>5</sub>O<sub>2</sub>) derived from  $MS^2$  spectrum, which allow to propose the formation of hydroperoxy derivative. Similarly, in the case of 185-B isomer, a favored loss of a H<sub>2</sub>O<sub>2</sub> molecule with the consequent formation of a species at  $m/z$  151.0865 (C<sub>8</sub>H<sub>11</sub>ON<sub>2</sub>) was observed and could be interpreted as a hydroperoxide derivative.

The structural assignment of hydroperoxy derivatives was based on the key losses of H<sub>2</sub>O<sub>2</sub> (34 Da) and H<sub>2</sub>O (18 Da), which are indicative of the formation of a peroxy bond [23,24]. The proposed mechanism for the formation of hydroperoxy derivative involves hydrogen abstraction (low step of the reaction) by the produced HO<sup>•</sup> followed by the very fast reaction with O<sub>2</sub> [25].

The TPs at [M + H]<sup>+</sup> at  $m/z$  201.0869 (two isomers 201-A,B) were detected, all derived by the hydroxylation of hydroperoxy TPs. This assignment is supported by the mass difference of 15.9948 from the

Table 3

Retention times and mass spectra characteristics of IPMP and its oxidation products by GC-MS.

| $R_t$ (min) | Product                                 | $m/z$ fragments (% relative intensity) | Similarity (%) |
|-------------|---|--|----------------|
| 11.45       | IPMP                                    | 152(47), 137(100), 124(35)             | 95             |
| 16.28       | 2-ethyl-3-methoxy pyrazine (P1)         | 138(100), 123(35), 137(37), 105(21)    | 89             |
| 11.63       | 1-(2-methoxy-3-pyrazinyl)-ethanone (P2) | 152(12), 137(41), 43(100)              | 75             |

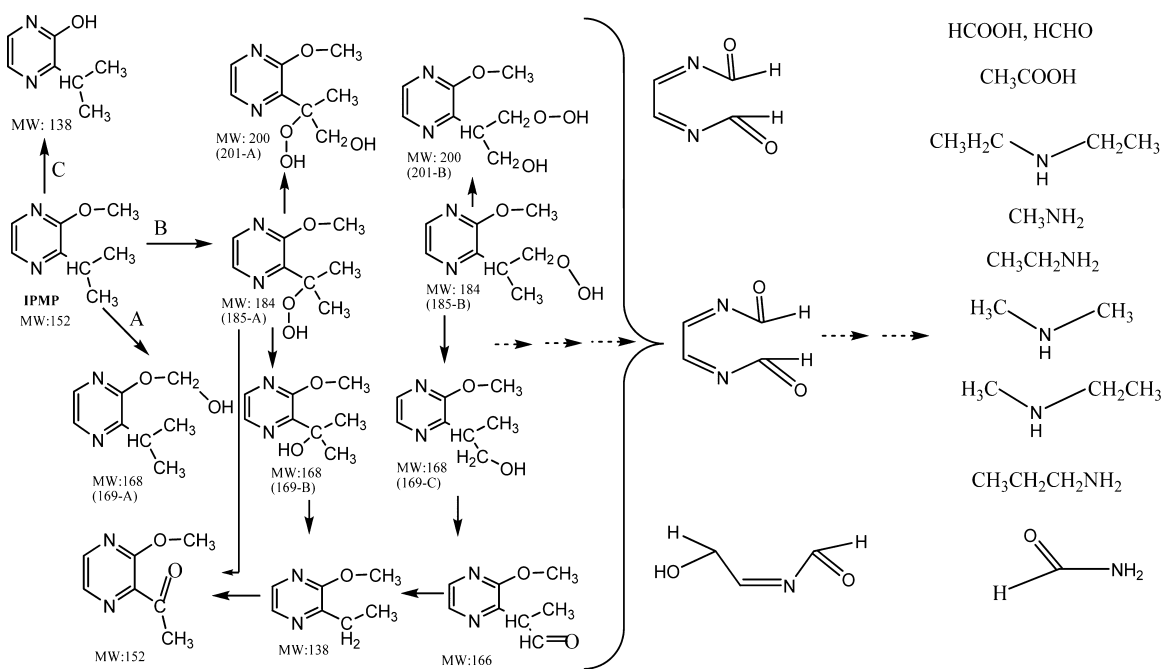


**Fig. 3.** Proposed degradation pathways of IPMP photocatalytic degradation in the presence of TiO<sub>2</sub> and simulated solar light.

parent compounds and the formation of MS<sup>2</sup> product ions at *m/z* 183.0755, which is consistent with the loss of a water molecule. The MS<sup>2</sup> and MS<sup>3</sup> spectra reveal also key fragment ions presented in Table 2 which come from a loss of methanol molecule, CO and formic acid and evidence the presence of hydroperoxy bond in the studied species [23,26]. The formation of a species at *m/z* 139.0866 and an empirical formula C<sub>7</sub>H<sub>11</sub>ON<sub>2</sub> invokes the cleavage of the methoxy group and the formation of 2-isopropyl-pyrazinol. Two TPs with *m/z* 153.0658 and 167.0807 sharing empirical formulas consistent with the oxidation of the isopropyl-group were also detected but it was not possible to accomplish a fragmentation study on these two TPs. However, the high resolution and accurate measurements, allowed to propose TPs structures which are depicted in Table 2.

The TP at *m/z* 153.0658 1-(2-methoxy)-3-pyrazinyl ethanone was detected using GC-MS, as well. One more intermediate arising from dealkylation of isopropyl chain, 2-ethyl-3-methoxy pyrazine was also eluted in 16.28 min by GC-MS system. The time evolution profiles of TPs in Fig. 2 show that all products attained their maximum concentrations within the same time scale (5–10 min) showing that the formation of hydroxy and hydroperoxy derivatives can take place simultaneously. Reduction and/or hydrolysis of the hydroperoxy derivatives could be also followed for the generation of the corresponding hydroxy derivatives [27]. On the other hand, the demethylated and oxidized TPs showed slower formation within 10 min of irradiation that could be formed after the HO<sup>•</sup> radical attack at the alkyl groups (Fig. 2). On the basis of the identification of intermediates, their evolution profile as well as the mineralization and scavenging studies, a tentative photocatalytic degradation pathway of IPMP was proposed in Fig. 3. The pathways include single hydroxylation that occurred mainly in the isopropyl chain (pathway A), HO<sup>•</sup> radical electrophilic attack with the subsequent O<sub>2</sub> addition (pathway B) and the cleavage of methoxy group (pathway C) bonds via positive holes. Although the high reactivity of hydroxyl radicals toward aromatic rings, dealkylation of the isopropyl side chain is one of the dominant processes. The proposed mechanism for photocatalytic degradation of isopropyl group involves reaction of a hydroxyl radical with either

the secondary or a primary carbon, which via the corresponding hydroperoxide leads to formation of aldehyde and keto structures [28]. The dealkylated intermediates were suggested to proceed via further oxidation of the keto TPs and subsequent decarboxylation reactions [22,28]. After successive dealkylation, all the above intermediates were further transformed by an oxidative opening of the aromatic ring via hydroxyl radicals and/or positive holes continuous attack, giving rise to the formation of lower molecular weight and more oxidized molecules as reported elsewhere [15,16] and depicted in Fig. 3.

As regards the organoleptic quality of TPs, no information is available on their taste and odor properties because all of them are new chemical entities. According to literature data, the majority of the identified TPs arising from MBT photocatalytic degradation holding the benzothiazole-moiety have been reported to pose threats to the esthetic value of the water [19]. Following the current state of knowledge for the degradation of mercaptobenzothiazole [19] and taking into account the fact that the identified TPs bearing the heterocyclic pyrazine ring, it is assumed that the TPs are potentially odor compounds contributing to the organoleptic quality of the water samples. However, all the identified TPs completely disappear very quickly after 30 min. This clearly proves the efficiency of heterogeneous photocatalysis for the degradation of the IPMP, rendering this process a sustainable treatment technology for taste and odor control.

### 3.4. Toxicity evaluation

Acute toxicity was evaluated by monitoring changes in the natural emission of the luminescent bacteria *V. fischeri* when challenged with toxic compounds and is expressed as percentage of inhibition of the bacteria luminescence. Toxicity (inhibition %) evolution during the photocatalytic treatment is depicted in Fig. 4. The initial toxicity of IPMP solution showed an initial inhibition of 19% that is slightly increases at 30 min of irradiation and reaching the value of 25%. It is worth mentioning that the highest toxicity is observed at irradiation times where the majority of the identified TPs attain almost their minimum concentration. Thus, the slight

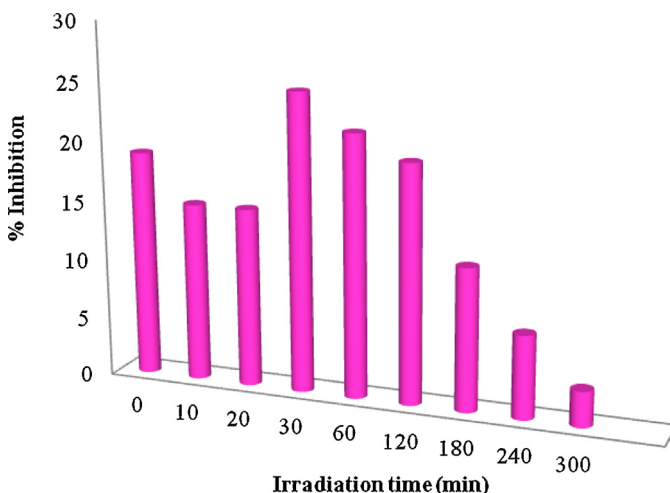


**Fig. 4.** % Inhibition of the marine luminescence bacteria *Vibrio Fischeri* as a function of photocatalytic treatment ( $[IPMP] = 10 \text{ mg L}^{-1}$ ,  $[\text{TiO}_2] = 100 \text{ mg L}^{-1}$ ,  $I = 600 \text{ W m}^{-2}$ ).

toxicity increase can be related to the generation of more toxic ring opened and/or aliphatic amine species during the photocatalytic treatment, while synergistic effects between them can also be considered. Quantifiable toxicity response of aliphatic amines to Microtox tests was reported elsewhere [29]. Obviously, bioluminescence inhibition values ranged always below 25%, which indicates that IPMP and its degradation products have low acute toxicity effects on the tested bacteria. Thereafter, inhibition % decreases leading to almost total detoxification after 300 min irradiation.

#### 4. Conclusions

The photocatalytic degradation of IPMP in the presence of  $\text{TiO}_2$  was investigated in detail focusing on the kinetic and mechanistic study. Results of the present study clearly point out that heterogeneous  $\text{TiO}_2$  photocatalytic treatment is suitable for the elimination of IPMP from the aqueous phase. Degradation for both IPMP and TOC followed pseudo-first order kinetic model. Scavenging studies indicated that  $\text{HO}^\bullet$  are responsible for the major degradation of IPMP whereas  $\text{O}_2^{\bullet-}$  and  $\text{h}^\bullet$  play also significant roles during the process. The photoinduced transformation of IPMP proceeded through the formation of numerous intermediate products and involved: hydroxylation, oxidation and demethylation pathways. Investigations on the intermediates suggest that the hydroxyl radical attack occur preferentially on the isopropyl chain of the IPMP before the ring opening and total mineralization. A significant abatement of the overall toxicity was accomplished as revealed by Microtox bioassay.

#### Acknowledgments

This research has been co-financed by the European Union (European Social Fund—ESF) and Greek National Funds through the Operational Program “Education and Lifelong Learning” of the National Strategic Reference Framework (NSRF)—Research Funding Program: Heracleitus II. Investing in knowledge society through the European Social Fund.

The authors would like to thank also the Unit of Environmental, Organic and Biochemical high resolution analysis-orbitrap-LC-MS analysis of the University of Ioannina for providing access to the facilities.

#### References

- [1] N. An, H. Xie, N. Gao, Y. Deng, W. Chu, J. Jiang, *Clean–Soil, Air, Water* (12) (2012) 1349–1356.
- [2] A. Peter, U. von Gunten, *Environ. Sci. Technol.* 41 (2007) 626–631.
- [3] C. Liang, D. Wang, M. Yang, W. Sun, S. Zhang, *J. Environ. Sci. Health, A* 40 (2005) 767–778.
- [4] A. Peter, O. Köster, A. Schildknecht, U. von Gunten, *Water Res.* 43 (2009) 2191–2200.
- [5] K. Zoschke, N. Dietrich, H. Börnick, E. Worch, *Water Res.* 46 (2012) 5365–5373.
- [6] L.A. Lawton, P.K.J. Robertson, R.F. Robertson, F.G. Bruce, *Appl. Catal., B: Environ.* 44 (2003) 9–13.
- [7] H. Tran, G.M. Evans, Y. Yan, A.V. Nguyen, *Water. Sci. Technol.* 9 (2009) 477–483.
- [8] E.E. Bamuza-Pemu, E.M.N. Chirwa, *Chem. Eng. Trans.* 24 (2011) 91–96.
- [9] M. Antonopoulou, E. Evgenidou, D. Lambropoulou, I. Konstantinou, *Water Res.* 53 (2014) 215–234.
- [10] L. Solorzano, *Limnol. Oceanogr.* 14 (5) (1969) 799–801.
- [11] M. Antonopoulou, A. Giannakas, Y. Deligiannakis, I. Konstantinou, *Chem. Eng. J.* 231 (2013) 314–325.
- [12] R. Palominos, J. Freer, M.A. Mondaca, H.D. Mansilla, *J. Photochem. Photobiol., A: Chem.* 193 (2008) 139–145.
- [13] S. Zheng, Y. Cai, K.E. O’Shea, *J. Photochem. Photobiol., A: Chem.* 210 (2010) 61–68.
- [14] M. Antonopoulou, V. Papadopoulos, I. Konstantinou, *J. Chem. Technol. Biotechnol.* 87 (2012) 1385–1395.
- [15] S. Horikoshi, H. Hidaka, *J. Photochem. Photobiol., A: Chem.* 141 (2001) 201–207.
- [16] F. Qi, B. Xu, Z. Chen, L. Feng, L. Zhang, D. Sun, *Chem. Eng. J.* 219 (2013) 527–536.
- [17] D. Fatta-Kassinos, M.I. Vasquez, K. Kümmeler, *Chemosphere* 85 (2011) 693–709.
- [18] D.A. Lambropoulou, I.K. Konstantinou, T.A. Albanis, A.R. Fernández-Alba, *Chemosphere* 83 (2011) 367–378.
- [19] F.B. Li, X.Z. Li, K.H. Ng, *Ind. Eng. Chem. Res.* 45 (2006) 1–7.
- [20] H.M. Maher, T. Awad, J. DeRuiter, C.R. Clark, *J. Chromatog. Sci.* 50 (2012) 1–9.
- [21] I. Losito, A. Amorisco, F. Palmisano, *Appl. Catal., B: Environ.* 79 (2008) 224–236.
- [22] M.V.P. Sharma, V.D. Kumari, M. Subrahmanyam, *Chemosphere* 72 (2008) 644–651.
- [23] M.-C. Reinnig, J. Warnke, T. Hoffmann, *Rapid Commun. Mass Spec.* 23 (2009) 1735–1741.
- [24] F. Giuffrida, F. Destaillats, L.H. Skibsted, F. Dionisi, *Chem. Phys. Lipids* 131 (2004) 41–49.
- [25] I.K. Konstantinou, T.M. Sakellarides, V.A. Sakkas, T. Albanis, *Environ. Sci. Technol.* 35 (2001) 398–405.
- [26] Y. Mochida, Y. Yokoyama, T. Kawai, S. Nakamura, M. Tsuchiya, *J. Mass Spectrom. Soc. Jpn.* 42 (1994) 207–215.
- [27] M.N. Möller, D.M. Hatch, H.-Y.H. Kim, N.A. Porter, *J. Am. Chem. Soc.* 134 (2012) 16773–16780.
- [28] E. Pelizzetti, C. Minero, V. Carlin, M. Vincenti, E. Pramauro, M. Dolci, *Chemosphere* 24 (1992) 891–910.
- [29] W.-L. Gong, K.J. Sears, J.E. Alleman, E.R. Blatchley, *Environ. Toxicol. Chem.* 23 (2004) 239–244.